DATA OF BRAZILIAN PASTURES AREAS MAPPING

Document elaborated by the Pasture Research Nucleus of the Image Processing and Geoprocessing Laboratory (Lapig) of the Federal University of Goiás (UFG), coordinated by professor Laerte Guimarães Ferreira. This and other methods relative to data production and pastures information are available in the Atlas of Pastures platform.

Goiânia, January 2022.

1. Overview

In the context of information produced by MapBiomas initiative purview, maps that describe the Brazilian land dynamic occupation by pastures in the last 36 years can be found (Collection 6).

This pasture mapping was based on the approach described by Parente et al. (2017, 2019) using satellite images from Landsat series and Random Forest monitored classifier (Breiman, 2001), as well as a wide feature space (Pasquarella et al., 2018), and solid statistic sample techniques (with the purpose of calibration and validation of the rating models) (figure 1).

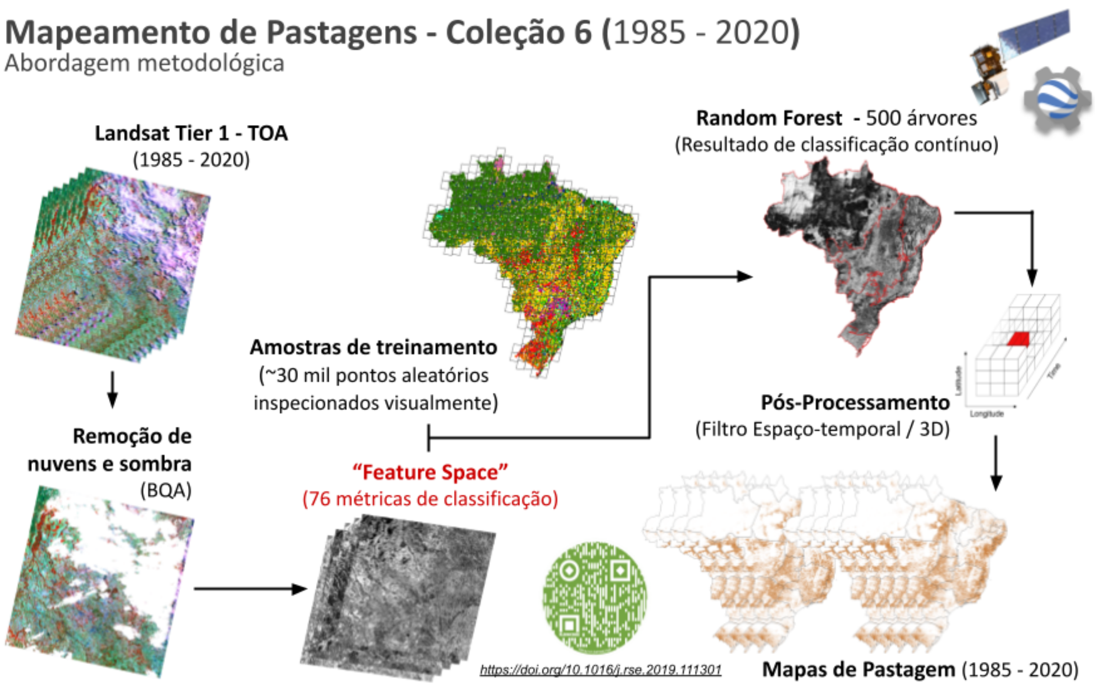

Figure 1. Fluxogram demonstrating the stage for mapping the pastures for Brazil.

2. Mapping approach

Our mapping approach considered as a rating unity the Landsat useful limits scenes (according to the World Reference System – WRS – 2 Orbits / Line without overlapping zones – figure 2) and a time window of 24 hours to the entire country, ensuring the prevalence of a specific year observation (the 2015 feature space considered images from the second semester of 2014 up to the first semester of 2016). This time window provided time series denser to the feature space generation, which was able to better capture the pastures vegetative vigor variations, since these areas are very susceptible to climate change (Ferreira et al., 2013).

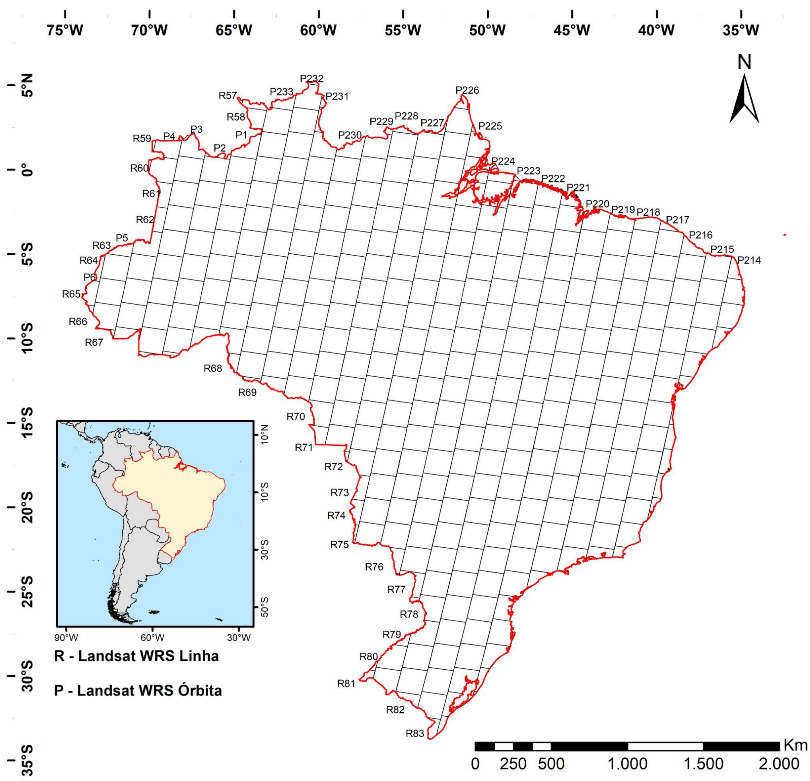

Figure 2. Landsat scenes (WRS) considered for the mapping of pasture areas between the years of 1985 to 2020.

The pasture mapping was produced with Landsat Collection 1 Tier 1 data, obtained between 1985 and 2020 (Markham & Helder, 2012). The Landsat 5 images were used on the first half of the time series (from 1985 to 1999). The images obtained by the Landsat 7 were considered only to the years 2000, 2001, 2002, and 2012. From 2003 to 2011 and 2013 to 2020, images from Landsat 5 and Landsat 8 were respectively used. These time series were normalized to the top of atmosphere (TOA) reflectance and selected according to the Landsat band quality assessment (Landsat 8 BQA = 2720 and Landsat 5/7 BQA = 672), in order to remove pixels contaminated by clouds and clouds shadow, as follows (figure 3)..

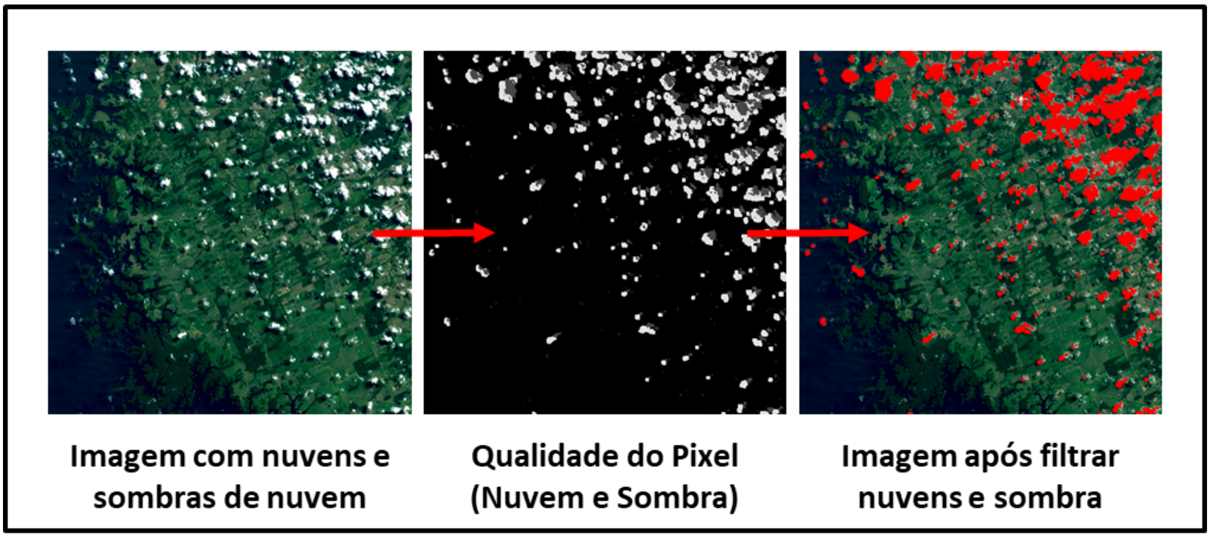

Figure 3. An example of the pixel by pixel removal process of cloud and shadow noise from each image used..

Due to Landsat images filtered with BQA and selected according to the established time period (24 months), five operations were applied (average, standard deviation, minimum, maximum, range, and percentiles) in six spectral bands (green, red, near infrared, short waves infrared 1, and short waves infrared 2), and three spectral indexes (Normalized Difference Vegetation Index – NDVI, Normalized Difference Water Index – NDWI (Gao, 1996), and Cellulose Absorption Index – CAI

(Nagler et al., 2003). Information of elevation and declivity were also considered, resulting from a Digital Elevation Model (DEM), and geographic coordinates. Our pasture mapping used 72 spectrum-time bands and four spatial metrics (table 1).

Table 1. *Feature space* utilized in the pasture classification (MapBiomas Colection 6), with a total of 72 com um total de 72 spectral-temporal metrics and four spatial metrics.

#	Bands / Indices	Operation	Period	Collection
1	Green	Mean	WET	3, 4, 5 e 6
2	Green	Standard Deviation	WET	3, 4, 5 e 6
3	Green	Minimum	WET	3, 4, 5 e 6
4	Green	Maximum	WET	3, 4, 5 e 6
5	Green	Amplitude	WET	3, 4, 5 e 6
6	Green	Percentile 10%	WET	5 e 6
7	Green	Percentile 25%	WET	5 e 6
8	Green	Percentile 75%	WET	5 e 6
9	Green	Percentile 90%	WET	5 e 6
10	Red	Mean	WET	3, 4, 5 e 6
11	Red	Standard Deviation	WET	3, 4, 5 e 6
12	Red	Minimum	WET	3, 4, 5 e 6
13	Red	Maximum	WET	3, 4, 5 e 6
14	Red	Amplitude	WET	3, 4, 5 e 6
15	Red	Percentile 10%	WET	5 e 6
16	Red	Percentile 25%	WET	5 e 6
17	Red	Percentile 75%	WET	5 e 6

18	Red	Percentile 90%	WET	5 e 6
19	NIR	Mean	WET	3, 4, 5 e 6
20	NIR	Standard Deviation	WET	3, 4, 5 e 6
21	NIR	Minimum	WET	3, 4, 5 e 6
22	NIR	Maximum	WET	3, 4, 5 e 6
23	NIR	Amplitude	WET	3, 4, 5 e 6
24	NIR	Percentile 10%	WET	5 e 6
25	NIR	Percentile 25%	WET	5 e 6
26	NIR	Percentile 75%	WET	5 e 6
27	NIR	Percentile 90%	WET	5 e 6
28	SWIR1	Mean	WET	3, 4, 5 e 6
29	SWIR1	Standard Deviation	WET	3, 4, 5 e 6
30	SWIR1	Minimum	WET	3, 4, 5 e 6
31	SWIR1	Maximum	WET	3, 4, 5 e 6
32	SWIR1	Amplitude	WET	3, 4, 5 e 6
33	SWIR1	Percentile 10%	WET	5 e 6
34	SWIR1	Percentile 25%	WET	5 e 6
35	SWIR1	Percentile 75%	WET	5 e 6
36	SWIR1	Percentile 90%	WET	5 e 6
37	SWIR2	Mean	WET	3, 4, 5 e 6
38	SWIR2	Standard Deviation	WET	3, 4, 5 e 6
39	SWIR2	Minimum	WET	3, 4, 5 e 6
40	SWIR2	Maximum	WET	3, 4, 5 e 6
41	SWIR2	Amplitude	WET	3, 4, 5 e 6

42	SWIR2	Percentile 10%	WET	5 e 6
43	SWIR2	Percentile 25%	WET	5 e 6
44	SWIR2	Percentile 75%	WET	5 e 6
45	SWIR2	Percentile 90%	WET	5 e 6
46	NDVI	Mean	WET	3, 4, 5 e 6
47	NDVI	Standard Deviation	WET	3, 4, 5 e 6
48	NDVI	Minimum	WET	3, 4, 5 e 6
49	NDVI	Maximum	WET	3, 4, 5 e 6
50	NDVI	Amplitude	WET	3, 4, 5 e 6
51	NDVI	Percentile 10%	WET	5 e 6
52	NDVI	Percentile 25%	WET	5 e 6
53	NDVI	Percentile 75%	WET	5 e 6
54	NDVI	Percentile 90%	WET	5 e 6
55	NDWI (Gao, 1996)	Mean	WET	3, 4, 5 e 6
56	NDWI (Gao, 1996)	Standard Deviation	WET	3, 4, 5 e 6
57	NDWI (Gao, 1996)	Minimum	WET	3, 4, 5 e 6
58	NDWI (Gao, 1996)	Maximum	WET	3, 4, 5 e 6
59	NDWI (Gao, 1996)	Amplitude	WET	3, 4, 5 e 6
60	NDWI (Gao, 1996)	Percentile 10%	WET	5 e 6
61	NDWI (Gao, 1996)	Percentile 25%	WET	5 e 6
62	NDWI (Gao, 1996)	Percentile 75%	WET	5 e 6
63	NDWI (Gao, 1996)	Percentile 90%	WET	5 e 6
64	CAI (Nagler *et al.*, 2003)	Mean	WET	3, 4, 5 e 6
65	CAI (Nagler *et al.*, 2003)	Standard Deviation	WET	3, 4, 5 e 6

66	CAI (Nagler *et al.*, 2003)	Minimum	WET	3, 4, 5 e 6
67	CAI (Nagler *et al.*, 2003)	Maximum	WET	3, 4, 5 e 6
68	CAI (Nagler *et al.*, 2003)	Amplitude	WET	3, 4, 5 e 6
69	CAI (Nagler *et al.*, 2003)	Percentile 10%	WET	5 e 6
70	CAI (Nagler *et al.*, 2003)	Percentile 25%	WET	5 e 6
71	CAI (Nagler *et al.*, 2003)	Percentile 75%	WET	5 e 6
72	CAI (Nagler *et al.*, 2003)	Percentile 90%	WET	5 e 6
73	SRTM (Farr *et al.*, 2007)	Elevation	-	5 e 6
74	SRTM (Farr *et al.*, 2007)	Slope	-	5 e 6
75	Geographic Coordinate	Latitude	-	5 e 6
76	Geographic Coordinate	Longitude	-	5 e 6

All the classified scenes were patchwork by year, resulting in a time series of maps of pastures probability. To improve these results, a space-time filter was applied, which was able to mitigate abrupt and sometimes unrealistic transitions using, simultaneously, information of both dimensions. The filter implemented by the SciPy catalog (Scipy, 2018), used a period of five years and 3 x 3 pixels to replace the kernel central value by the medium of 45 probability values (figure 4). Upon this result, a limit of 51% was applied (Parente et al., 2019), to produce Brazilian pasture maps

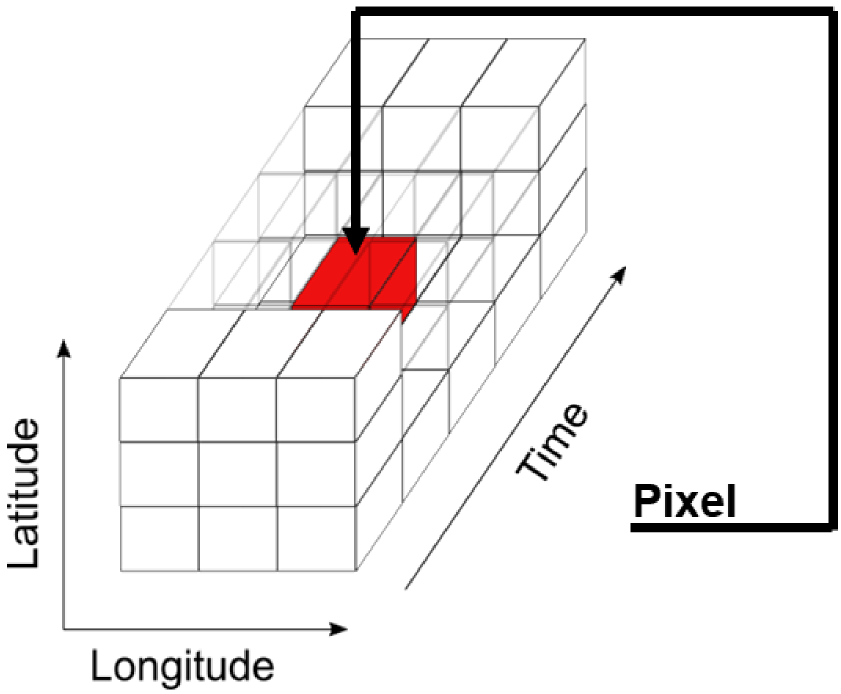

Figure 4. Illustration of the multidimensional filter technique used for mapping pastures. It is performed in space (3x3 pixels) and time (5 years) a filtering with the use of a kernel 3D of 3x3x 5.

An independent quality assessment was performed considering 5000 validation points. The design sampling also considered a pasture map from 2015 (Parente et al., 2017), in a way that the random point numbers could be balanced by class (2500 to "pasture" class and 2500 to "non pasture" class), conservatively assuming that the mapping's minimum accuracy was 50% and the assessment error was 1% in a 95% of confidence interval (Lohr, 2009).

The validation sampling was evaluated by five examiners, but to be considered in the accuracy evaluation, it was necessary to have four or more agreement points (in other words, at least four examiners identified the same land coverage and class of use), resulting in (at least) 4100 available samples to each year. To all pasture maps, the overall, producer, and user accuracy were assessed by a balanced confusing matrix, which removes the sampling bias (Pontius & Millones, 2011).

The pasture mapping presented a ~ 91% of overall accuracy, ~ 95% of user accuracy (from 2000 onwards), and a producer accuracy varying between 60% and 72%, indicating an oversight error prevalence for all the years.

References

BREIMAN, L. Random forests. Machine learning, v. 45, n. 1, p. 5-32, 2001.

FARR, T. G., et al. (2007), The Shuttle Radar Topography Mission, Rev. Geophys., V45

GAO, B.C. NDWI – A Normalized Difference Water Index for remote sensing of vegetation liquid water from space. Remote Sensing of Environment, v.58, p.257-266, 1996.

LOHR, S.L. Sampling: Design and Analysis, 2 edition. ed. Cengage Learning, Boston, Mass, 2009.

MARKHAM, B. L.; STOREY, J. C.; WILLIAMS, D. L.; IRONS, J. R. Landsat sensor performance: history and current status. Geoscience and Remote Sensing, IEEE Transactions on, v. 42, n. 12, p. 2691-2694, 2004.

MARKHAM, B. L.; HELDER, D. L. Forty-year calibrated record of earth-reflected radiance from Landsat: A review. Remote Sensing of Environment, v. 122, p. 30-40, 2012.

NAGLER, P. L.; INOUE, Y.; CLENN, E. P.; RUSS, A. L.; DAUGHTRY, C. S. T. Cellulose absorption index (CAI) to quantify mixed soil-plant litter scenes. Remote Sens Environ, v. 87, pp. 310–325, 2003.

PARENTE, L.; FERREIRA, L.; FARIA, A.; NOGUEIRA, S.; ARAÚJO, F.; TEIXEIRA, L.; HAGEN, S. Monitoring the brazilian pasturelands: A new mapping approach based on the landsat 8 spectral and temporal domains. International Journal of Applied Earth Observation and Geoinformation, v. 62, p. 135-143, 2017.

PARENTE, L.; FERREIRA, L.. Assessing the Spatial and Occupation Dynamics of the Brazilian Pasturelands Based on the Automated Classification of MODIS Images from 2000 to 2016. Remote Sensing, v. 10, n. 4, p. 606, 2018.

PARENTE, L.; MESQUITA, V.; MIZIARA, F.; BAUMANN, L.; FERREIRA, L. Assessing the pasturelands and livestock dynamics in Brazil, from 1985 to 2017: A novel approach based on high spatial resolution imagery and Google Earth Engine cloud computing. Remote Sens. Environ. 2019, 232, 111301.

PASQUARELLA, V. J.; HOLDEN, C. E.; WOODCOCK, C. E. Improved mapping of forest type using spectral-temporal Landsat features. Remote Sensing of Environment, v. 210, p. 193-207, 2018.

PONTIUS JR, R. G.; & MILLONES, M. Death to Kappa: birth of quantity disagreement and allocation disagreement for accuracy assessment. International Journal of Remote Sensing, v. 32, n. 15, p. 4407-4429, 2011.

SCIPY. Reference Guide - SciPy v1.1.0. Available online: https://docs.scipy.org/doc/scipy-1.1.0/reference/generated/scipy.ndimage.median.html (accessed on 01 August 2018).

WANG, J.; ZHAO, Y.; LI, C.; YU, L.; LIU, D.; GONG, P. Mapping global land cover in 2001 and 2010 with spatial-temporal consistency at 250 m resolution. ISPRS Journal of Photogrammetry and Remote Sensing, v. 103, p. 38-47, 2015.